

The stability of Lomer–Cottrell jogs in nanopillars

Christopher R. Weinberger^{a,*} and Wei Cai^b

^aSandia National Laboratories, P.O. Box 5800, MS1411, Albuquerque, NM 87185-1411, USA

^bDepartment of Mechanical Engineering, Stanford University, CA 94305-4040, USA

Received 20 October 2010; revised 15 November 2010; accepted 20 November 2010

Available online 26 November 2010

Single arm spiral sources, or truncated Frank–Read sources, have been used frequently to interpret the size dependent plasticity in micropillars. The basis for these sources is strong pinning points which have been proposed to exist based on immobile Lomer–Cottrell jogs. Here, we show, using molecular dynamics of face-centered cubic nanopillars, that Lomer–Cottrell jogs are not as immobile as initially thought and that they do not provide strong pinning points for single arm sources.

© 2010 Acta Materialia Inc. Published by Elsevier Ltd. All rights reserved.

Keywords: Dislocations; Micropillar; Jog; Plastic Deformation

Experiments on pillars ranging in sizes from a few hundred nanometers to tens of micrometers have shown that the flow stress in the pillars increases as pillar size decreases [1–3]. The plastic deformation of these pillars must occur through the activation of dislocation sources, which increase in strength as the pillar diameter decreases. Two competing mechanisms have emerged to explain the experimental observations: dislocation starvation [4] and single arm sources [5]. The dislocation starvation model maintains that mobile dislocations escape the crystals, leaving them starved of mobile dislocations, and plasticity continues with nucleation from the surface. The single arm source model claims that truncated Frank–Read sources control plasticity and the strengthening is caused by shorter source lengths in smaller volumes. However, this model requires strong pinning points and the nature of these pinning points is unclear.

The single arm source model is primarily supported by dislocation dynamics (DD) simulations [6,7] and some experiments [8]. These DD simulations require strong pinning points, which are created by dislocation segments, or junctions, which are assumed to be immobile. In order to provide a theoretical basis for single arm sources, Lee and Nix [9] investigated the creation of strong pinning points from Lomer–Cottrell (LC) junctions in face-centered cubic (fcc) micropillars. They concluded that LC junctions can indeed form single arm

sources by transforming into LC jogs but rely on the immobility of the jog. In this letter, we investigate the stability and mobility of LC jogs and evaluate their potential as single arm sources.

In order to ensure that our atomistic models are appropriate to simulate the dynamics of Lomer–Cottrell jogs, we first need to verify that the interatomic potentials used in this study reproduce known properties of these dislocations. For example, Mills et al. [10] have shown that different embedded atom model potentials will predict both compact and planar cores for Lomer dislocations. To this end, we have computed the core structure of both Lomer dislocations, the compact core as shown in Figure 1a, and the Lomer–Cottrell dislocation, which has a dissociated core structure shown in Figure 1b. The core structure for the predicted Lomer dislocation matches observations in aluminum [11] and the Lomer–Cottrell dislocation core structure shows the expected dissociation. These dislocations are known to have high Peierls stresses [12] and thus low mobility on their {001} glide planes, which is accurately predicted by the potentials we use [13,14] exhibiting Peierls stresses in the GPa range. However, LC jogs, which are the subject of investigation in this letter, are different from the Lomer and LC dislocations because they have two end nodes, one of which is always constricted [9], about which the dislocation arms can rotate.

To investigate the stability of LC jogs, we use molecular dynamics simulations. This is done by introducing a jog into a dislocation that spans a nanopillar, as shown in Figure 2a. Most of the nanopillars in our simulations have a diameter of 16 or 30 nm, while a few have a

*Corresponding author. Tel.: +1 505 284 0896; e-mail addresses: crweinb@sandia.gov; caiwei@stanford.edu

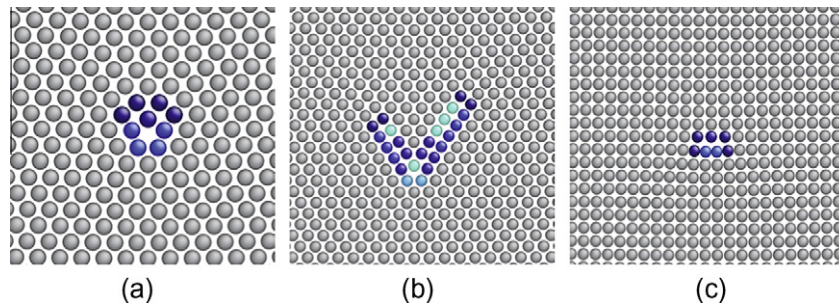


Figure 1. The dislocation core for (a) a Lomer dislocation, (b) a Lomer–Cottrell Lock and (c) a 45° mixed dislocation on a $\{100\}$ plane. The atoms are colored by the centro-symmetry deviation parameter and the material shown here is copper.

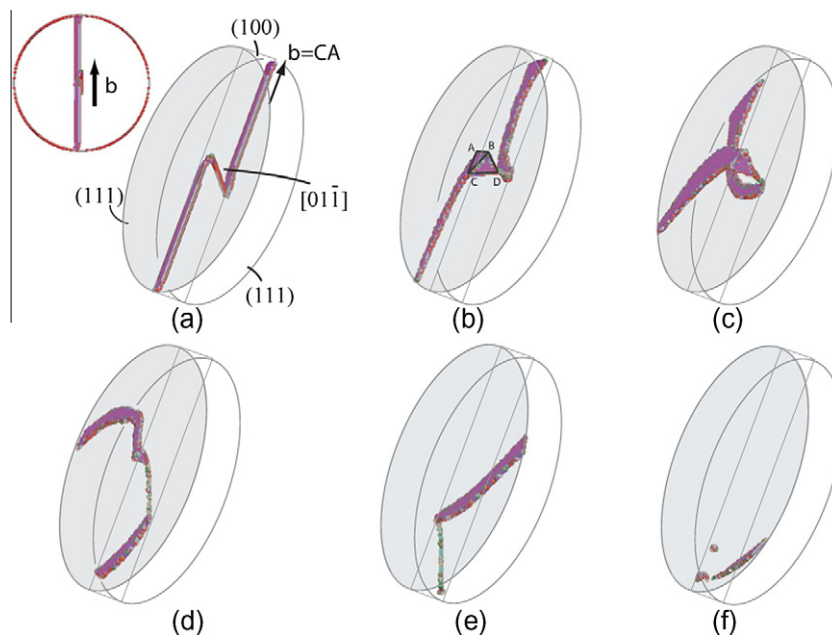


Figure 2. The operation of a single arm source created from a Lomer–Cottrell jog and its dissolution in a 30 nm diameter nickel nanopillar with a jog length of $30\frac{a}{2}\langle 110\rangle$. (a) The initial configuration of the source showing both an end-on view of the pillar with surface atoms present and a perspective view of the initial source at 0 ps. (b) The extended node readily forms as predicted from geometrical considerations at 4 ps. (c) The arms rotate past each other on their $\{111\}$ planes at 10 ps. The jog rotates on its $\{100\}$ plane, eliminating the extended node and forming a constricted jog along the whole jog length (d) (18 ps). (e) The dislocation structure drifts along the $\{100\}$ plane at 40 ps and (f) eventually leaves the nanopillar at 48 ps. Movies of this simulation can be found online in the supplemental information.

diameter of 50 nm, with lengths twice the diameter of the pillars (see [movies 1–4 in Supplemental Information](#)). The pillars have free side surfaces and a circular cross-section with periodic boundary conditions along their length. The jog length in most of the simulations is $15\frac{a}{2}\langle 110\rangle$; however, doubling the jog length in the 30 nm diameter pillars showed no significant change in the jog behavior. Two different orientations are studied, $\langle 100\rangle$ and $\langle 111\rangle$. The $\langle 100\rangle$ nanopillars are loaded with a compressive stress along their axis while the $\langle 111\rangle$ are loaded by applying a shear stress to the pillar. Pure shear stresses are applied to the pillar instead of compressive loading in order to provide a driving force on the mobile dislocations on the $\{111\}$ plane. The stability of the LC jog is studied under both constant stress (0 MPa, 500 MPa and 1 GPa) and constant strain (0% and 3%) and at both 300 and 0 K except for the 50 nm pillars, which we only study at 300 K and 1 GPa. The effect of stacking fault energy is included in the study

using the Foiles–Hoyt [13] potential for nickel and Mishin [14] potential for copper, which predict different dissociation widths (with a ratio of 1:1.8) and different minimum-energy core structures. The Lomer dislocation has lower energy in the nickel potential and the Lomer–Cottrell dislocation has lower energy in the copper potential.

For $\langle 100\rangle$ oriented nanopillars, two basic behaviors are observed which are determined by the magnitude of the applied load. If the applied axial load is above a critical stress, the dislocation is able to escape when the arms rotate and constrict the nodes of the LC jog, allowing the jog to rotate on its glide plane, as shown in [Figure 2](#). The initial condition is a screw dislocation dissociated on a $\{111\}$ plane with an LC jog connecting the two arms, as shown in [Figure 2a](#). Under the applied axial load (1 GPa here), we see the arms begin to rotate ([Fig. 2b](#)). One node of the LC jog is extended and the other is constricted ([Fig. 2b](#)), similar to that predicted

by Lee and Nix [9]. However, at this point the constriction has already spread partway along the jog. As the arms continue to rotate (Fig. 2c and d), we see that the LC jog changes to a constricted core eliminating the extended node (Fig. 2d and e). Lee and Nix predicted a dissociated core structure with constrictions at both ends, but here we observe that the core is constricted along its whole length. If the arms were to rotate 180° from this configuration, the extended core structure would often not return (as is observed in other simulations), but rather the jog would remain constricted. This is because the Lomer dislocation is apparently able to rotate on its $\{100\}$ glide plane out of the edge configuration. The new orientation does not intersect $\{111\}$ planes, preventing dissociation onto $\{111\}$ type planes. The dislocation is able to freely move along the $\{100\}$ plane, as shown in Figure 2e, to which the jog is confined, and eventually the jog escapes, as shown in Figure 2f. The rotation and constriction of the LC jog, which facilitate escape, are features observed in all of our simulations, illustrating the mobility of these dislocation structures.

If the applied stress is below the activation stress of the source, the dislocation immediately reorients itself, eliminating the LC jog. The LC dislocation again begins to rotate on the $\{100\}$ plane while extending its length and reducing the length of the dissociated screw dislocations. The driving force for the reorientation is line tension since the energy of the dislocation can be reduced by reducing its total line length through the lengthening of the jog. Line tension provides the necessary torque to reorient the jog, so that this mechanism is not related to the pillar size. Furthermore, the applied load, in this orientation, has no resolved shear stress on the glide plane of the jog and thus provides no driving force for the reorientation. The only two dislocations in the jog structure that experience glide forces from the applied loads are the Shockley partials, which both have Schmid factors of 0.24.

In some cases, the dislocation is able to escape within the short simulation time. In all the simulations the LC jog is able to rotate in its $\{100\}$ plane, illustrating that the reorientation of the jog is not an artifact of the high stresses in the previous simulations. Similar to the high stress cases, the reorientation and loss of the strong pinning points originate from the ability of the LC jog to reorient from its edge orientation to a mixed dislocation on the $\{100\}$ plane.

Additional simulations were performed for $\langle 111 \rangle$ oriented nanopillars to ensure the generality of the

observed behavior. In this case, the dislocation arms that should act as single arm sources are oriented perpendicular to the pillar axis. Thus, as the arms rotate, their line length does not change significantly; this may, perhaps, increase their stability. The applied shear stress, on the $\{111\}$ plane in the x -direction, provides no resolved shear stress on the $\{100\}$ glide plane of the LC jog. Similar to the $\langle 100 \rangle$ orientation, simulations at 300 and 0 K under constant stress and strain were performed. However, despite the geometry changes, the behavior is quite similar to that observed in the $\{100\}$ pillars. The results for a 30 nm nickel pillar at 300 K and zero applied stress is shown in Figure 3. The behavior is typical of low stress simulations. The initial condition shows the pillar with two screw dislocation arms and an LC jog (Fig. 3a). The jog begins to reorient (Fig. 3b) by rotating in the $\{100\}$ plane as it consumes one of the arms. The arm that is consumed was originally connected to the constricted node, as the extended node is clearly shown in the figure. Finally, we see that the $\{100\}$ dislocation is now stretched over most of the pillar, thus reducing its line energy and eliminating its potential as a single arm source. At high stresses, the jog loss is similar to the $\langle 100 \rangle$ orientation.

To further understand the mobility of dislocations on $\{100\}$ planes in fcc crystals, which have been reported as slip systems in aluminum at high temperatures [15], we performed quasi-static calculations of the Peierls stress and core structure of 45° mixed dislocations. The mobility of mixed dislocations on $\{100\}$ planes is important because, if they are not mobile, rotation out of the LC jog orientation would still provide strong pinning points. Since the edge dislocations, or Lomer and Lomer–Cottrell dislocations, have non-planar cores and high Peierls stresses and screw dislocations should dissociate onto $\{111\}$ planes and become highly mobile, we use the 45° mixed dislocation as a test case for mobility of mixed dislocations on $\{100\}$ planes. The core structure of these dislocations is shown in Figure 1c, which is planar in nature. This suggests that mixed dislocations on the $\{100\}$ should be significantly more mobile than edge dislocations. The Peierls stresses of the two different metals are 145 and 65 MPa for nickel and copper, respectively. We note that these values are significantly lower than those obtained for dislocations oriented in the LC direction. Thus, once the dislocation is able to rotate out of the LC orientation, it is able to glide and exit the pillar.

These molecular dynamics simulations show that LC jogs are more mobile than initially thought. None of our

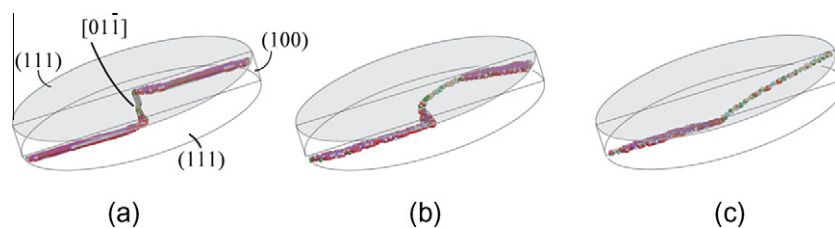


Figure 3. The dissolution of an LC jog in a $\{111\}$ oriented 30 nm diameter nickel nanopillar under zero applied stress. (a) The initial jog structure where the arms are perpendicular to the pillar axis. (b) The constricted node extends the dislocation on the $\{100\}$ plane, reorienting the dislocation away from edge under line tension forces at 3 ps. (c) The $\{100\}$ dislocation has extended all the way to the free surface, effectively eliminating the jog at 9 ps. Movies of this simulation can be found online in the supplemental information.

simulations show a stable single arm source. These jogs are unstable in nanopillars when the arms begin to rotate, which suggests they are unable to provide strong pinning points in micro- and submicrometer pillars. The origin of strong pinning points that create single arm sources is unclear. It is possible that impurities may segregate to dislocation cores and pin the dislocations, which may explain the observations of single arm sources observed in some experiments [8]. However, from these results it is doubtful that dislocation structures such as LC jogs are inherently strong enough to create the necessary pinning points and permanent dislocation sources by themselves. These results also point to the necessity of performing additional molecular dynamics studies on the stability of dislocation structures that may give rise to single arm sources.

This research was supported in part by an appointment to the Sandia National Laboratories Truman Fellowship in National Security Science and Engineering, sponsored by Sandia Corporation (a wholly owned subsidiary of Lockheed Martin Corporation) as Operator of Sandia National Laboratories under its U.S. Department of Energy Contract No. DE-AC04-94AL85000. The work was partly supported by National Science Foundation Career Grant CMS-0547681 and the Army High Performance Computing Research Center at Stanford.

Supplementary data associated with this article can be found, in the online version, at [doi:10.1016/j.scriptamat.2010.11.037](https://doi.org/10.1016/j.scriptamat.2010.11.037).

- [1] M. Uchic, D. Dimiduk, J. Florando, W. Nix, *Science* 305 (2004) 986.
- [2] J.R. Greer, W.C. Oliver, W.D. Nix, *Acta Mater.* 52 (2005) 1821.
- [3] D. Dimiduk, M. Uchic, T.A. Parthasarathy, *Acta Mater.* 53 (2005) 4065.
- [4] J. Greer, W. Nix, *Phys. Rev. B* 73 (2006) 245410.
- [5] S. Rao, D. Dimiduk, T. Parthasarathy, M. Uchic, M. Tang, C. Woodward, *Acta Mater.* 56 (2008) 3245.
- [6] H. Tang, K. Schwarz, H. Espinosa, *Phys. Rev. Lett.* 100 (2008) 185503.
- [7] C. Motz, D. Weygand, J. Senger, P. Gumbsch, *Acta Mater.* 57 (2009) 1744.
- [8] S. Oh, M. Legros, D. Kiener, P. Gruber, G. Dehm, *Acta Mater.* 55 (2007) 5578.
- [9] S.-W. Lee, W.D. Nix, *Mater. Eng. Sci. A* 527 (2010) 1903.
- [10] M.J. Mills, M.S. Daw, S.M. Foiles, *Ultramicroscopy* 56 (1994) 79.
- [11] M.J. Mills, P. Stadelman, *Philos. Mag.* 60 (1989) 355.
- [12] D. Rodney, *Phys. Rev. B* 76 (2007) 144108.
- [13] S.M. Foiles, J.J. Hoyt, *Acta Mater.* 54 (2006) 3351.
- [14] Y. Mishin, M. Mehl, D. Papaconstantopoulos, A. Voter, J. Kress, *Phys. Rev. B* 63 (2001) 224106.
- [15] J.P. Hirth, J. Lothe, *Theory of Dislocations* Krieger (1982).